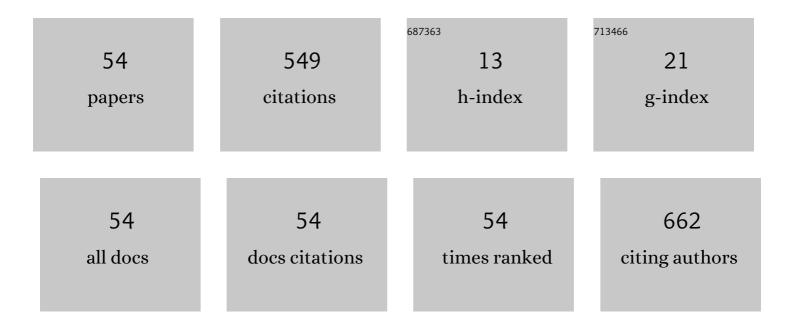
Marcio Daldin Teodoro

List of Publications by Year in descending order

Source: https://exaly.com/author-pdf/4099016/publications.pdf Version: 2024-02-01



#	Article	IF	CITATIONS
1	Connecting morphology and photoluminescence emissions in β-Ag2MoO4 microcrystals. Ceramics International, 2022, 48, 3740-3750.	4.8	9
2	Tailoring Bi2MoO6 by Eu3+ incorporation for enhanced photoluminescence emissions. Journal of Luminescence, 2022, 243, 118675.	3.1	9
3	Spin-dependent analysis of homogeneous and inhomogeneous exciton decoherence in magnetic fields. Physical Review B, 2022, 105, .	3.2	0
4	α Ag2WO4 under microwave, electron beam and femtosecond laser irradiations: Unveiling the relationship between morphology and photoluminescence emissions. Journal of Alloys and Compounds, 2022, 903, 163840.	5.5	3
5	Diffusion of Photoexcited Holes in a Viscous Electron Fluid. Physical Review Letters, 2022, 128, 136801.	7.8	9
6	YVO4:RE (RE = Eu, Tm, and Yb/Er) nanoparticles synthesized by the microwave-assisted hydrothermal method for photoluminescence application. Ecletica Quimica, 2022, 47, 39-49.	0.5	2
7	Tuning intrinsic defects in ZnO films by controlling the vacuum annealing temperature: an experimental and theoretical approach. Physica Scripta, 2022, 97, 075811.	2.5	1
8	Cation-exchange mediated synthesis of hydrogen and sodium titanates heterojunction: Theoretical and experimental insights toward photocatalyic mechanism. Applied Surface Science, 2021, 538, 148137.	6.1	25
9	Effect of hydrothermal temperature on the antibacterial and photocatalytic activity of WO3 decorated with silver nanoparticles. Journal of Sol-Gel Science and Technology, 2021, 97, 228-244.	2.4	8
10	Comparison of Aβ (1–40, 1–28, 11–22, and 29–40) aggregation processes and inhibition of toxic specie generated in early stages of aggregation by a water-soluble ruthenium complex. Journal of Inorganic Biochemistry, 2021, 215, 111314.	es 3.5	7
11	Synthesis, characterization, photocatalytic, and antimicrobial activity of ZrO2 nanoparticles and Ag@ZrO2 nanocomposite prepared by the advanced oxidative process/hydrothermal route. Journal of Sol-Gel Science and Technology, 2021, 98, 113-126.	2.4	15
12	Structure, Photoluminescence Emissions, and Photocatalytic Activity of Ag ₂ SeO ₃ : A Joint Experimental and Theoretical Investigation. Inorganic Chemistry, 2021, 60, 5937-5954.	4.0	10
13	Magnetic and power tuning of spin-asymmetric multiple excitons in a GaAs quantum well. Physica E: Low-Dimensional Systems and Nanostructures, 2021, 129, 114599.	2.7	1
14	Spin relaxation of holes in In0.53Ga0.47As/InP quantum wells. Physica E: Low-Dimensional Systems and Nanostructures, 2021, 131, 114700.	2.7	1
15	Optical Mapping of Nonequilibrium Charge Carriers. Journal of Physical Chemistry C, 2021, 125, 14741-14750.	3.1	7
16	Suppression of vapor-liquid-solid (VLS) mechanism in the growth of α-Sb2O4 nanobelts by a vapor-deposition approach. Materials Science in Semiconductor Processing, 2021, 134, 106006.	4.0	2
17	Unraveling the relationship between bulk structure and exposed surfaces and its effect on the electronic structure and photoluminescent properties of Ba0.5Sr0.5TiO3: A joint experimental and theoretical approach. Materials Research Bulletin, 2021, 143, 111442.	5.2	7
18	Quantitative Correlation Study of Dislocation Generation, Strain Relief, and Sn Outdiffusion in Thermally Annealed GeSn Epilayers. Crystal Growth and Design, 2021, 21, 1666-1673.	3.0	14

#	Article	IF	CITATIONS
19	Electron–phonon coupling enhancement and displacive magnetostructural transition in SrCr2 As2 under magneto-Raman spectroscopy. Journal of Physics Condensed Matter, 2021, 33, 105401.	1.8	2
20	Multi-dimensional architecture of Ag/α-Ag ₂ WO ₄ crystals: insights into microstructural, morphological, and photoluminescence properties. CrystEngComm, 2020, 22, 7903-7917.	2.6	9
21	Insights into the nature of optically active defects of ZnO. Journal of Luminescence, 2020, 227, 117536.	3.1	15
22	Influence of the metastable state (<i>V</i> ++) on the electronic properties of SnO2 nanowires under the influence of light. Journal of Applied Physics, 2020, 128, .	2.5	8
23	Microwave-Driven Hexagonal-to-Monoclinic Transition in BiPO ₄ : An In-Depth Experimental Investigation and First-Principles Study. Inorganic Chemistry, 2020, 59, 7453-7468.	4.0	24
24	Metallic behavior in STO/LAO heterostructures with non-uniformly atomic interfaces. Materials Today Communications, 2020, 24, 101339.	1.9	1
25	Growth and formation mechanism of shape-selective preparation of ZnO structures: correlation of structural, vibrational and optical properties. Physical Chemistry Chemical Physics, 2020, 22, 7329-7339.	2.8	23
26	Enhanced degradation of the antibiotic sulfamethoxazole by heterogeneous photocatalysis using Ce0,8Gd0,2O2-Î/TiO2 particles. Journal of Alloys and Compounds, 2019, 808, 151711.	5.5	25
27	Magnetically controlled exciton transfer in hybrid quantum-dot–quantum-well nanostructures. Physical Review B, 2019, 100, .	3.2	1
28	Role of defects on the enhancement of the photocatalytic response of ZnO nanostructures. Applied Surface Science, 2018, 448, 646-654.	6.1	46
29	Direct preparation of standard functional interfaces in oxide heterostructures for 2DEG analysis through beam-induced platinum contacts. Applied Physics Letters, 2018, 113, .	3.3	2
30	Recombination dynamics of Landau levels in an InGaAs/InP quantum well. Physical Review B, 2018, 98, .	3.2	0
31	Atmosphere-Dependent Photoconductivity of ZnO in the Urbach Tail. International Journal of Photoenergy, 2018, 2018, 1-8.	2.5	9
32	Aharonov-Bohm Effect for Neutral Excitons in Quantum Rings. Nanoscience and Technology, 2018, , 255-280.	1.5	0
33	Photocurrent enhancement and magnetoresistance in indium phosphide single nanowire by zinc doping. Journal Physics D: Applied Physics, 2018, 51, 255106. Electroluminescence on-off ratio control of <mml:math< td=""><td>2.8</td><td>2</td></mml:math<>	2.8	2
34	xmlns:mml="http://www.w3.org/1998/Math/MathML"> <mml:mrow><mml:mi mathvariant="italic">n<mml:mtext mathvariant="italic">â^^</mml:mtext><mml:mi mathvariant="italic">i<mml:mtext mathvariant="italic">â^^</mml:mtext><mml:mi mathvariant="italic">nâ^^<mml:mi< td=""><td>3.2</td><td>6</td></mml:mi<></mml:mi </mml:mi </mml:mi </mml:mrow>	3.2	6
35	structures. Physical Review B, 2018, 98, . Investigation of trapping levels in p-type Zn3P2nanowires using transport and optical properties. Applied Physics Letters, 2018, 112, 193103.	3.3	12
36	Recombination kinetics of photogenerated electrons in InGaAs/InP quantum wells. Journal of Applied Physics, 2016, 119, 094301.	2.5	2

Marcio Daldin Teodoro

#	Article	IF	CITATIONS
37	Optical and transport properties correlation driven by amorphous/crystalline disorder in InP nanowires. Journal of Physics Condensed Matter, 2016, 28, 475303.	1.8	1
38	Probing semiconductor confined excitons decay into surface plasmon polaritons. Applied Physics A: Materials Science and Processing, 2016, 122, 1.	2.3	3
39	Carrier transfer in vertically stacked quantum ring-quantum dot chains. Journal of Applied Physics, 2015, 117, .	2.5	15
40	Structural and magnetic confinement of holes in the spin-polarized emission of coupled quantum ring–quantum dot chains. Physical Review B, 2014, 90, .	3.2	10
41	Low temperature magneto-photoluminescence of GaAsBi /GaAs quantum well heterostructures. Journal of Applied Physics, 2014, 115, 123518.	2.5	11
42	Temperature driven three-dimensional ordering of InGaAs/GaAs quantum dot superlattices grown under As2 gas flux. Applied Surface Science, 2014, 305, 689-696.	6.1	3
43	Aharonov-Bohm Effect for Neutral Excitons in Quantum Rings. Nanoscience and Technology, 2014, , 247-265.	1.5	1
44	In-plane mapping of buried InGaAs quantum rings and hybridization effects on the electronic structure. Journal of Applied Physics, 2012, 112, .	2.5	12
45	Magneto-optical properties of Cd1â^'xMnxS nanoparticles: influences of magnetic doping, Mn2+ ions localization, and quantum confinement. Physical Chemistry Chemical Physics, 2012, 14, 3248.	2.8	27
46	Analysis of confinement potential fluctuation and band-gap renormalization effects on excitonic transition in GaAs/AlGaAs multiquantum wells grown on (100) and (311)A GaAs surfaces. Physica B: Condensed Matter, 2012, 407, 2131-2135.	2.7	4
47	Anisotropic Confinement, Electronic Coupling and Strain Induced Effects Detected by Valence-Band Anisotropy in Self-Assembled Quantum Dots. Nanoscale Research Letters, 2011, 6, 56.	5.7	10
48	Isotropic Hall effect and "freeze-in―of carriers in the InGaAs self-assembled quantum wires. Journal of Applied Physics, 2011, 110, .	2.5	14
49	Alignment and optical polarization of InGaAs quantum wires on GaAs high index surfaces. Materials Letters, 2011, 65, 1427-1430.	2.6	3
50	Carrier transfer in the optical recombination of quantum dots. Physical Review B, 2011, 83, .	3.2	6
51	Aharonov-Bohm Interference in Neutral Excitons: Effects of Built-In Electric Fields. Physical Review Letters, 2010, 104, 086401.	7.8	80
52	Contrasting LH-HH subband splitting of strained quantum wells grown along [001] and [113] directions. Physical Review B, 2010, 81, .	3.2	5
53	Interface roughness scattering in laterally coupled InGaAs quantum wires. Applied Physics Letters, 2010, 97, 262103.	3.3	14
54	Substrate orientation effect on potential fluctuations in multiquantum wells of GaAsâ^•AlGaAs. Journal of Applied Physics, 2008, 103, 093508.	2.5	13